Crossover between Rayleigh-Taylor instability and turbulent cascading atomization mechanism in the bag-breakup regime

Nicolas Rimbert, Guillaume Castanet

Crossover between Rayleigh-Taylor instability and turbulent cascading atomization mechanism in the bag-breakup regime

Nicolas Rimbert and Guillaume Castanet
Nancy University LEMTA, ESSTIN, 2 avenue de la Forêt de Haye, F-54504 Vandoeuvre-lès-Nancy cedex, France

The question of whether liquid atomization depends on instability dynamics (through refinements of Rayleigh-Plateau, Rayleigh-Taylor, or Kelvin-Helmholtz mechanisms) or on turbulent cascades, as suggested by Richardson and Kolmogorov, is still open. In this paper, experimental results reveal that both mechanisms are needed to explain the probability density functions (PDFs) of the droplets in a spray obtained from an industrial fan spray nozzle. Instability of Rayleigh-Taylor type controls the size of the largest droplets while the smallest droplets follow a PDF given by a turbulent cascading mechanism characterized by a log-Lévy stable law that has a stability parameter equal to 1.70. This value is very close to the inverse value of the Flory exponent and can be related to a recent model developed by N. Rimbert for intermittency modeling stemming from self-avoiding random vortex stretching.

I. INTRODUCTION

Log-normal probability density functions (PDFs) are used by experimental analysts in many fields. In spray atomization, Kolmogorov was the first to explain their widespread appearance. In his modeling of turbulent atomization [1], he devised a discrete Markov process converging toward a lognormal PDF. Later Obukhov [2] used log-normal PDFs to describe the statistical distribution of intermittent dissipation in turbulent flows. In turn, this approach has been employed by Kolmogorov [3] in his famous K62 modeling of turbulence intermittencies. Since these pioneering works, turbulence intermittencies have been the subject of considerable attention, and Frisch's book [4] gives an excellent overview of the main contributions to this field.

While Schertzer and Lovejoy [5] emphasized the role of the log-stable law in turbulent-linked geophysics as universal multifractals (thanks to a generalized central limit theorem), Kida [6,7] explained empirically the statistical laws of turbulence intermittencies with a log-stable law of stability parameter 1.65. Although this remains the subject of some debate [8], recent advances in this field can be found in Refs. [9,10] wherein Kida's results are discussed and validated through a self-avoiding random vortex stretching process. In this modeling, the topological constraint of nonintersection, applied to a vortex tube, forces the value of the stability parameter to be the inverse value of Flory's exponent (i.e., 1/.588 or 1.70), a scaling exponent well known in polymer physics [11]. As a result, the stable law is proved to be fully asymmetric to the left, and Rimbert [12] was able to find a relation between its scale parameter and the important scale of turbulent flows, that is, Kolmogorov's and Taylor's scales.

In regard to turbulent atomization modeling, few improvements have been made since Kolmogorov's aforementioned work [1]. While experimentalists still base their work on a variety of empirical laws [12], some of which are close to the log-normal law (such as the upper limit log-normal Evans law or the log-Weibull law), theoreticians have widened their views to include log-infinitely-divisible distributions [13], multifractal analysis [14], or refinements of Kolmogorov first modeling [15]. In Ref. [16], it was shown that log-stable laws are also a good choice when modeling some turbulent spray PDFs. This is only a brief summary, and more detailed reviews about atomization and its representation through statistical distributions can be found in [12,17,18].

The aim of this paper is to demonstrate on the basis of spray PDFs that turbulent cascading can play a significant role in the atomization in the bag-breakup regime. However, while multistep cascading mechanisms are widely used to describe turbulent intermittencies, it is questionable whether this kind of mechanism is relevant to the modeling of the atomization. For instance, there are numerous records of primary atomization and secondary atomization, but there is no evidence of successive fragmentations having three (or even more) steps except in the very-high-velocity phenomenon known as catastrophic breakup [19]. This may be related to the fact that after two breakup events, air becomes trapped in the vicinity of the droplets in what is often called the *added mass*; that is, the shear stress at the droplet surface finally vanishes due to the progressive transfer of momentum to the gas phase. Recently, evidence has been found that a cascading mechanism can be appropriate [20] for high-speed sprays (e.g., more than 60 m/s air velocity for an air blast atomizer).

At moderate liquid velocity, most analyses made in the nonturbulent regime are based on instability theory. It usually involves a competition among surface tension effect (Rayleigh-Plateau mechanism), acceleration of a droplet in the ambient air (Rayleigh-Taylor mechanism), and shear instability appearing on the edge of the droplet (Kelvin-Helmholtz mechanism. For a review of these classical instabilities, see [21]. In a recent study of the so-called nonturbulent bag-breakup regime [22], the Rayleigh-Taylor mechanism was widely used to explain experimental results.

In the present study, dealing with an industrial nozzle in the bag-breakup regime, Rayleigh-Taylor (RT) instability is used to explain the first stage of the breakup. However, the analysis shows that a turbulent cascade mechanism also seems to be necessary to describe the appearance of finer droplet PDFs that would result from the burst of the bag. To some extent, this

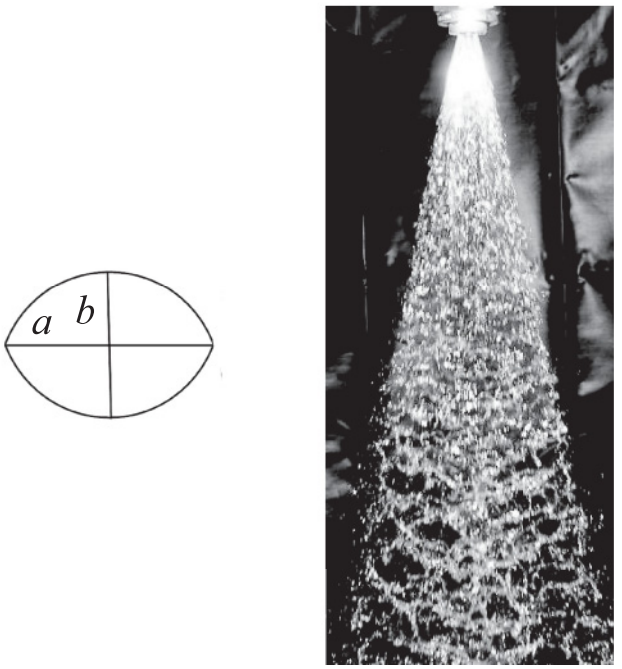

FIG. 1. Sketch of the nozzle orifice and photograph of the experimental setup (Lechler nozzle ref. 665-042, 8 bars). The orifice of the nozzle is made up of two identical circular segments pieced together ($2a = 977$ μm and $2b = 646$ μm for ref. 665-042).

can be related to the late stage of the turbulent mixing in the Rayleigh-Taylor instability, where recently a Kolmogorov-like cascading scenario has been used (see [23] for a description of the one-phase RT instability developing between a hot gas and a cold gas and [24] for a review of corresponding debates on RT instability).

II. EXPERIMENTAL SETUP

The experimental setup was devised to test several kinds of industrial nozzles, and we focus on results obtained with a 665-042 Lechler nozzle. Its aperture is shown in Fig. 1, and it is made of two identical circle segments pieced together. Its equivalent radii r_{eq} are equal to 452 μm. The nominal flow rate is around 80 L of water per minute depending on the inlet pressure, which is either 8 bar (in Fig. 1) or 15 bar (everywhere else) in this study.

The measurements were obtained using a phase Doppler anemometer (PDA) from Dantec Dynamics. The spray was illuminated by two crossing laser beams coming from a Continuous Wave (CW) Nd:Yag laser at 532 nm. In addition to the droplet size, the vertical droplet velocity was measured. The measurement of the droplet velocity is similar in its principle to the classical laser Doppler velocimetry technique (LDV) and the size measurement can be seen an extension of this latter technique [25]. Droplet sizing is based on the measurement of the phase difference of the Doppler burst observed by detectors positioned under different light scattering angles.

In our experimental setup, the probe volume formed by the intersection of the laser beams was roughly an ellipsoid of dimensions 600 μm $\times$ 600 μm $\times$ 4000 μm. The PDA was used in the refraction mode and therefore, to minimize the contribution of reflection rays, the PDA receiver was positioned at 73° in the forward scattering direction. Based on optical considerations that account for a 2π ambiguity on the phase of the detector signals [25], the PDA system is expected to measure droplet sizes up to about 1800 μm. This limit does not account for the fact that bigger droplets may saturate the photomultiplier tubes (PMTs) used as detectors, while the smaller droplets may not trigger the detection for the same threshold levels and the same high voltages of the PMT. In practice, this phenomenon can reduce the effective range of droplet size measurement. In the present study, care was taken to configure the measurement system so that small drops resulting from the bag breakup were accurately resolved, but this was achieved to the detriment of the detection of the larger droplets. Due to the Gaussian shape of the laser beams, light intensity is less important on the edge of the probe volume than at its center. For this reason, the larger droplets were mostly detected when they were passing on the edge of the measurement volume given that otherwise they would have saturated the detectors and would have been rejected in the signal processing. This is illustrated in Fig. 2. While the droplets had nearly the same axial velocity U whatever their size, namely about 41 m/s (see Fig. 3), their transit time in the measurement volume fell drastically after 400 μm, which indicates that the frequency of droplets above 400 μm was underestimated. In contrast, droplets ranging from 10 to 400 μm had an average transit time very close to half the maximum transit time $TT_{\max} = \frac{(600)\times 10^{-6}}{U} \approx 14$ μs (the transit time of a droplet crossing the measurement volume along its center line), indicating that the experimental parameters (laser intensity, PMT high voltage, detection thresholds) were well adjusted for the detection of the majority of these droplets. As PDA is able to measure the size and the velocity of each droplet simultaneously, it is possible to derive from the experimental data a joint size-velocity PDF as presented in Fig. 3.

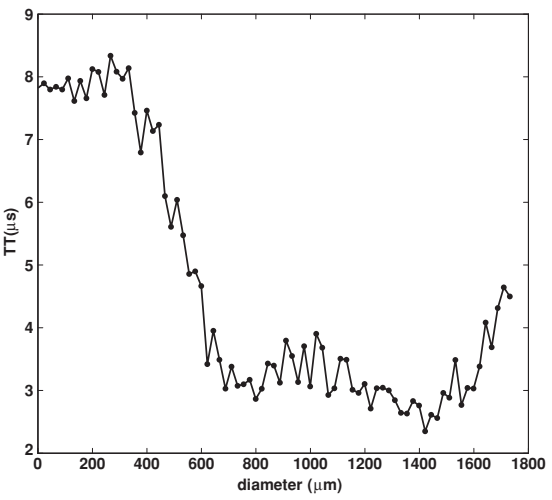

FIG. 2. Comparison of average measured transit times, showing that the larger droplets are mostly detected on the edge of the measurement volume.

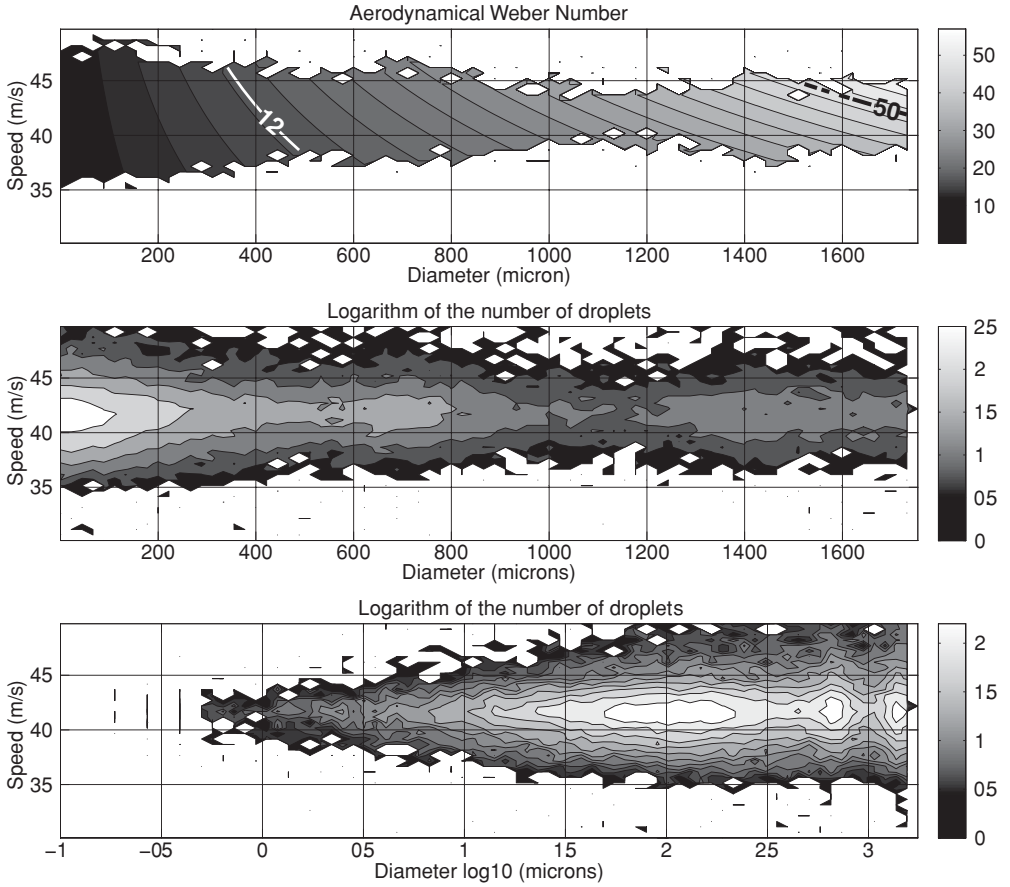

FIG. 3. Experimental size-velocity PDF (Lechler nozzle ref. 665-122, 15 bars, 4 cm below the exit). (a) The domain of the bag breakup (12 $<$ We $<$ 50) is delimited. Comparison between the frequency distribution of the droplet velocity and diameter (b) and the distribution of the velocity and magnitude $\log_{10}$ (d), (c). A large amount of droplets are located under 100 μm, which is in the aerodynamic stability domain.

III. EXPERIMENTAL RESULTS

The nondimensional parameters governing the stability of a droplet in an air stream are the (aerodynamic) Weber number and the Ohnesorge number, defined by

$$\mathrm{We}_{\mathrm{aero}} = \frac{\rho_G U^2 d}{\gamma} \quad \text{and} \quad \mathrm{Oh} = \frac{\mu_L}{\sqrt{\gamma \rho_L d}}, \tag{1}$$

where ρ_G and ρ_L stand respectively for the air density and the water density, γ is the air-water surface tension, μ_L is the liquid dynamic viscosity, and d is the droplet diameter. According to [26], when the Ohnesorge number is low (i.e., mainly for liquids with low viscosity) and the Weber number is less than 12, the droplet is aerodynamically stable, whereas a Weber number in the range of 12–50 indicates that the droplet is likely to break up in what is called a bag breakup (cf. Fig. 4). In Fig. 3(a), isocontour lines of the Weber number are given in the velocity-diameter plane for data collected 4 cm below the nozzle (first measurement position).

From this figure, it can be seen that most droplets on the millimeter scale are located in the bag-breakup regime, whereas droplets with a diameter less than 400 μm are aerodynamically stable. The facts that droplets of every size flowed at almost the same speed and that all the droplets' size-velocity PDFs were roughly the same shape on the vertical axis seem to indicate that, apart from initial bag breakups,

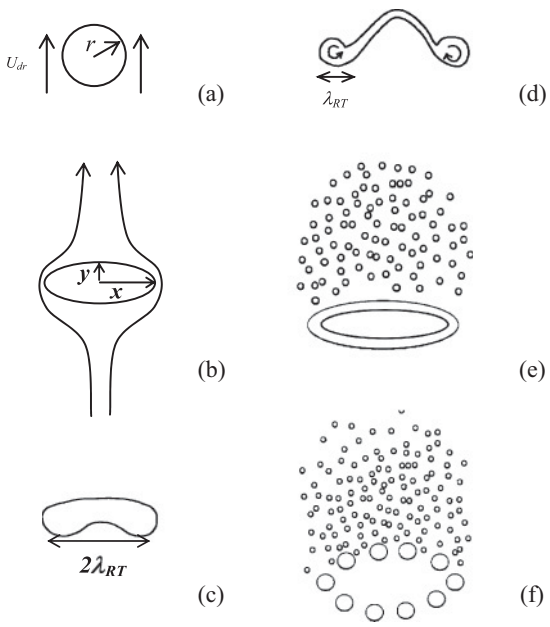

FIG. 4. Six stages of the bag breakup (cf. [23]): (a) The droplets result from the Rayleigh-Plateau mechanism. (b) They elongate in the relative air flow. (c) This results in a Rayleigh-Taylor wave and (d) in the formation of a ring and a bag. (e) the blowup of the bag and (f) of the ring leads to a bimodal distribution.

droplets were subsequently not submitted to any particular shear from the ambient air. Otherwise, this would have resulted in a lower velocity for the smaller droplets. This also suggests that the air within the spray was largely set in motion by the dispersed phase due to momentum transfers. Indeed, air movements were clearly noticeable in the vicinity of the spray during experiments. Consequently, Weber's number given by (2) is certainly overestimated because the velocity of water U shall be replaced by the drift velocity U_{dr} between the water droplet and air. If true, this means that apart from primary or secondary breakup, which are discussed below, droplets of any size are stable in the air flow.

Figure 3(b) represents the joint velocity-diameter PDF while Fig. 3(c) corresponds to the joint velocity-magnitude PDF (magnitude is here defined as the decimal logarithm of the diameter, magnitude 0 standing for 1-μm droplets). In Fig. 3(c), three peaks can be noticed, each of them corresponding to a peculiar physical mechanism. The three peaks in the distribution are found to be 1355 μm (magnitude 3.13), 661 μm (magnitude 2.82), and roughly 100 μm (more precisely 200 μm, considering the Sauter mean diameter of the bag). Statistics were collected from more than 50,000 droplets. Since all droplets have roughly the same velocity, we considered this figure is sufficient to obtain converged results in terms of number of droplets per class of size and velocity.

Figure 4 shows the main steps in the classical mechanism for bag breakup (cf. [19] for more detail). Six stages are used generally:

After the breakup of the core fluid into droplets out of the nozzle orifice, which could be explained qualitatively by the Rayleigh-Plateau theory [Fig. 4(a)], the droplet still undergoes surface deformations and perturbations [Fig. 4(b)]. These result ultimately in the emergence of the Rayleigh-Taylor instability [Fig. 4(c)] in which the droplet transforms into a rim and a bag [Fig. 4(d)].

The bag bursts [Fig. 4(e)], followed soon by the rim [Fig. 4(f)]. An idea of the characteristic times of these phenomena can be found in [26–28]. Figure 5 shows the marginal magnitude PDF obtained from the joint velocity magnitude PDF. From right to left, it can be supposed that the first peak corresponds to unburst droplets created by the Rayleigh-Plateau instability, while the second peak corresponds to droplets resulting from the fragmentation of the rim. The third peak corresponds to the cloud of droplets created by the bursting of the bag. This interpretation seems to be confirmed by the fact that the Sauter mean diameter d_{32} of the bag droplets is about 200 μm, resulting in the ratio

$$\frac{d_{32}^{(\mathrm{bag})}}{d^{(\mathrm{init})}} = \frac{200}{1350} \approx 0.148, \tag{2}$$

which is also very close to the value 0.14 reported in [19] and [21]. It should be noted that the numbers of droplets corresponding to the peaks cannot be compared. For the reasons explained in Sec. II, the detection rate by the PDA is dependent on the droplet size, especially above 600 μm.

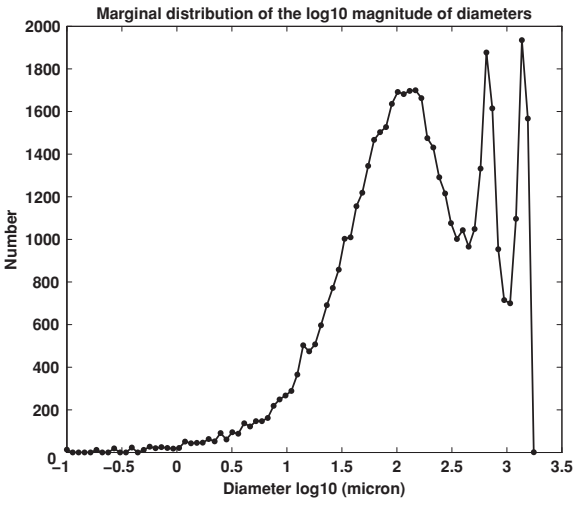

FIG. 5. Marginal size distribution (Lechler nozzle ref. 665-122, 15 bars, 4 cm below the exit). From right to left, the first peak is the peak of the initial droplets, the second peak is given by the Rayleigh-Taylor theory, while the third peak is the bag-breakup peak.

A. Rayleigh-Taylor breakup

In Fig. 5, the ratio between the diameter of the mother droplet and the diameter of the rim droplets appears to be very close to 2 (almost 0.3 in magnitude scale). An explanation for this can be developed on the basis of the Rayleigh-Taylor theory as prescribed in [19]. A first attempt was made by Kytschtka *et al.* [29], although this did not take the deformation of the droplet into account. The deformation of the droplet was introduced for the first time in O'Rourke's work [30] in the so-called Taylor analogy breakup (TAB) model, but this only takes the elastic surface vibration of the droplet and its viscous damping into account in a spring-dashpot model, and no reference is made to Rayleigh-Taylor instability. Parameters of the model are obtained from dimensional analysis. A more sophisticated approach to droplet deformation [31,32] corresponds to the so-called droplet deformation and breakup (DDB) model. In this model, the influence of droplet deformation on the trajectory and the drag coefficient is taken into account, and the reduced equations are obtained through energy-related variational techniques. Two ordinary differential equations (ODEs) must be solved, one for the droplet deformation and the other for the droplet position. The breakup is assumed to occur at the end of the deformation phase, which is shown experimentally to correspond to a deformation rate close to 2 [31]. Here again, the exact breakup mechanism is left undetermined. In the work discussed below, we supposed that this latter hypothesis was valid and that the mother droplet was deformed into an oblate spheroid of major and minor semiaxes x and y [Fig. 4(b)] when the Rayleigh-Taylor-induced breakup starts. At the final stage of the deformation, $x \ll y$ so the droplet can be assimilated to a disk. Since the Reynolds number of the droplet is relatively high (typically Re $>$ 1000), the drag coefficient C_d is almost a constant equal to 1.7 for incompressible flow [19]. Note that this value is greater than the value of 1.2, which corresponds to the limit case of an infinitely thin disc at high Reynolds number.

The condition upon which a wave will ultimately split the droplet in two parts (the rim and the bag) can be specified. This wave should have a wavelength equal to the major semiaxis. As in [33], we assume that results of the classical two-dimensional (2D) instability theory can be extended to the three-dimensional (3D) case. With this hypothesis, in the

Rayleigh-Taylor theory, it can be demonstrated that the fastest growing wavelength is expressed as follows:

$$\lambda_{\mathrm{RT,\,max}} = 2\pi\sqrt{\frac{3\gamma}{f\Delta\rho}}, \tag{3}$$

where f is the deceleration of the disc in the air stream, expressed as

$$f = \frac{3}{8}\frac{\rho_G}{\rho_L}\frac{x^2}{r^3}C_d U^2, \tag{4}$$

where r is the initial radius of the droplet so that

$$\frac{\lambda_{\mathrm{RT,max}}}{r} = 2\pi\left(\frac{r}{x}\right)\sqrt{\frac{8\gamma}{C_d\rho_G U^2 r}}. \tag{5}$$

The condition $x = \lambda_{\mathrm{RT,\,max}}$ leads to

$$\left(\frac{x}{r}\right)^4 = 32\pi^2\frac{\gamma}{\rho_G C_d U^2 r} \simeq 9.1. \tag{6}$$

From Fig. 5, r is about 675 μm for the peak of the largest droplet. Given $\rho_G = 1.3$ kg/m^3, $U = 41$ m/s, $C_d = 1.7$, and $\gamma = 0.072$ N.m^{-1}, the Reynolds number $\mathrm{Re} = Ud/\nu_G = 1800$ and the Weber number based on the initial diameter [given by Eq. (1)] is $\mathrm{We} = 41$. Using Eq. (6), it appears that the deformation should reach $x \approx 1.74\,r$, so that the deceleration can be high enough for a Rayleigh-Taylor wave of fastest growth to cut the drop in half. According to the DDB theory, when the ratio x/r is larger than 1, the maximum deformation is given by

$$\frac{x}{r} = \frac{\mathrm{We}}{6\pi}. \tag{7}$$

In the example, the maximum deformation is obtained for $x/r \approx 2.2$, so we may conclude that a Rayleigh-Taylor-induced breakup can actually occur for the considered droplets.

Since a deformation criterion for the bag breakup is $x/r = 2 = \lambda/r$ (see the experimental results in [30,31]), the approach described above can be used to draw more general conclusions. For instance, this criterion allows estimating a lower bound for the Weber number $\mathrm{We}_{\mathrm{min}}$ when a droplet can split in two equally sized droplets.

$$\left(\frac{x}{r}\right)^4 = 2^4 = 16 = 64\pi^2\frac{1}{C_d\mathrm{We}_{\mathrm{min}}}, \tag{8}$$

and finally

$$\mathrm{We}_{\mathrm{min}} = \frac{4\pi^2}{C_d} \approx 23.2, \tag{9}$$

which is consistent with Hinze's measurement for free-falling drops [12]. Some of Hinze's measurements were performed in a shock tube. In these kinds of compressible flows, the limit drag coefficient can be as high as $C_d = 3$ [19] instead of $C_d = 1.7$. Using Eq. (11), we find that this leads to $\mathrm{We}_{\mathrm{min}} = 13$, which was the value found experimentally by Hinze. This simple model is also very useful for evaluating the ring-to-bag volume ratio. In Fig. 4(c), it can be seen that the droplet is split into three parts by the two inflexion points of the wavy surface and therefore that two thirds of the drop come to the rim and one third come to the bag. Previous measurement of the rim to mother droplet volume ratio [32] gave a value of 70%, which is very close to the proposed 66%. Moreover, the rim, which contains two thirds of the volume, should break in appreciatively $n = 2/3(d_{\mathrm{mother}}/d_{\mathrm{daughter}})^3 \approx 16/3 \approx 5$ to 6 daughter droplets, which corresponds with the results reported in [32]. However, this is a one-dimensional (1D) analysis compatible with measurements on the breakup of a long cylinder in a crossflow. By making the same assumption with axisymmetric geometry, the volume ratio between the rim and the bag turns out to be 75/25%, which is closer to the other observed value of 80/20% [28].

Lastly, it should be noted that the condition $2x = 3\lambda_{\mathrm{RT}}$ (i.e., three waves growing on the disc surface) leads to the equation

$$\left(\frac{x}{r}\right)^4 = 12^2\pi^2\frac{1}{C_d\mathrm{We}}, \tag{10}$$

and setting $x = 2r$ leads to the minimum value

$$\mathrm{We}_{\mathrm{min}} = \frac{144\pi^2}{16C_d} = 52 \tag{11}$$

for the onset of the so-called bag-and-stamen or umbrella breakup.

In conclusion, this quite simple model suggests that the Weber number in the bag breakup ranges between 23 and 52, which is consistent with some previous measurements. This is also compatible with the shape of the spray PDF in our study because only the largest peaks are in this range.

B. Turbulent cascade and reagglomeration mechanism

During the preceding events, numerous tiny droplets were produced as a result of the burst of the bag. Their size distribution is very wide (see Fig. 5) and greatly different from the first two narrow peaks. This section is devoted to the analysis of the distribution of these fragments.

The main idea in the following is that this distribution is comparable to the widespread distribution of vortices in turbulent flows, a phenomenon known as intermittencies. In [10], a detailed scenario of turbulent intermittencies was devised using a self-avoiding random vortex stretching mechanism, which ultimately resulted in a log-stable distribution of vortices. In a highly classic way, the size of the most common vortices is given by the Taylor microscale while the size of the smallest vortices is given by the Kolmogorov scale. The log-stable distribution is defined by four parameters, which are evaluated both theoretically and experimentally. It should be restated at this point that it is impossible, except for a given set of parameters, to express stable distribution in analytic form. Only the analytic form of their Fourier transform (i.e., their characteristic function) is known, and there are several (actually an infinite number of) ways to characterize them. In this study, the definition of Samorodnitsky and Taqqu has been used [34]:

"A random variable X is said to have a stable distribution denoted $L_\alpha(x;\beta,\sigma,\delta)$ if there are real parameters $0 < \alpha \leqslant 2$, $0 < \sigma$, $-1 \leqslant \beta \leqslant 1$ and δ such that its characteristic function has the following form:

$$\hat{p}_\alpha(k;\beta,\sigma,\delta) = \exp(ik\delta - \sigma^\alpha|k|^\alpha[1 + i(\mathrm{sgn}(k))\beta\omega(|k|,\alpha)]) \tag{12}$$

where

$$\omega(|k|,\alpha) = \begin{cases} \tan(\alpha\pi/2) & \text{if } \alpha \neq 1 \\ -(2/\pi)\log|k| & \text{if } \alpha = 1 \end{cases}.$$

The most important parameter of these distributions is the stability index α (which is equal to 2 for Gaussian distribution and 1 for Cauchy distribution, as they are special cases, admitting an analytical form of stable distributions). As stable laws can be skewed either to the left or right, a skewness parameter β whose value range between –1 and 1 is the second parameter. Lastly, the scale parameter σ and the shift parameter δ are the closest to the standard deviation and the mean of normal Gaussian distribution, but they can first differ (when defined) and, second, strongly depend on the chosen form of the characteristic function. In [10], when applied to turbulence intermittency modeling, they were found to be $\alpha = 1.70$ (theoretically) and 1.69 (experimentally) for the stability index, $\beta = -1$ for the asymmetry parameter (both theoretically and experimentally, the resulting distributions are said to be totally skewed to the left), the scale parameter is given by

$$\sigma^{\alpha}_{\ln\varepsilon} = \ln\left(\frac{\lambda}{\eta}\right), \tag{13}$$

and the shift parameter $\delta_{ln\varepsilon}$ is given by the average dissipation of turbulent kinetic energy per unit volume and is therefore related to the large scale of the flow.

In the present study, it was quite difficult to make an *a priori* estimation of the different scales of turbulence. Nevertheless, reference values for the turbulent kinetic energy and the large scale were required and are available, in [35], for example. Here are some estimates for the turbulent kinetic energy dissipation ε, the Taylor scale λ, and the Kolmogorov scale η:

$$\varepsilon \cong \frac{u'^3}{L_{\text{int}}} \cong \frac{2^3}{1350 \times 10^{-6}} \cong 5900\ \text{m}^2/\text{s}^3, \tag{14}$$

$$\lambda = \sqrt{20\nu\frac{k}{\varepsilon}} \simeq 137\ \mu\text{m}\,(\text{magnitude } 2.13), \tag{15}$$

$$\eta \cong \left(\frac{\nu^3}{\varepsilon}\right)^{1/4} \cong 3\ \mu\text{m}\,(\text{magnitude } 0.48). \tag{16}$$

The fluctuating velocity order of magnitude, u', has been estimated to be around 2 m/s using velocity standard deviations of data of Fig. 3 and by fitting a Gaussian velocity distribution on the different size classes of droplets. The integral length L_{int} has been taken equal to the initial size of the mother droplet. Note that since exponents of formulas (15) and (16) are small, the result is not very sensitive to these, somewhat arbitrary, choices.

It should be noted that the value of the turbulent fluctuating velocity inside the liquid phase was identified with the rms fluctuation of the droplet's velocity and was therefore equally likely to represent the fluctuation of air velocity. In doing this, the value of turbulence dissipation rate ε may have been underestimated. However, it is apparent that the resulting Taylor microscale corresponds to the magnitude of the most common droplets (Fig. 6). Droplet sizes below the estimated Kolmogorov scale are also shown in Fig. 5 but they are

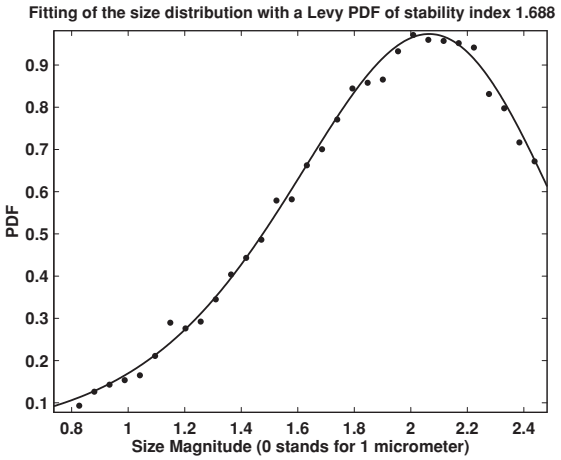

FIG. 6. The bag-breakup wide peak is fitted with a log-stable distribution of stability parameter close to 1.69.

not particularly numerous. While their presence could be related to the underestimation of the turbulence dissipation, it could also be linked to measurements errors with the PDA technique. The possibility of detecting such very small droplets is very unlikely due to the weakness of their scattered light. One explanation could be that there is a risk with the PDA technique that droplets larger than 1.8 mm may be interpreted as very small due to a 2π phase ambiguity on the phase measurement. There are obviously errors in measuring droplet size with the phase Doppler technique. In our study, the risks of errors were mainly due to the measurement-volume effect (MVE). The phase Doppler method is sensitive to particle trajectory effects that cause a phase error under Gaussian beam illumination. Because of the Gaussian shape of the laser beams, for some positions of the droplet within the measurement volume (formed by the intersection of the laser beams), the chosen scattering mode which should have been predominant in the direction of the detector in the case of plane waves may be of the same order of magnitude (or even less) as the other scattering modes, which are generally of secondary importance. Errors result therefore from the interference between reflected and refracted rays from the particle because only the dominant mode for a plane wave is considered by the PDA in the data processing. The bias on the size measurement may be important when the droplet is large and exceeds the size of the measurement volume. The MVE is a well-known problem with the phase Doppler technique and has already been the subject of comment by many authors. In the measurement system (classic PDA probe, Dantec Dynamics), this issue was addressed by means of a threshold in the data validation and by adding a third detector. If the phase ratios and the amplitude ratios of the three detection units are not within the expected tolerance, the measured phase will be invalid. This method is not perfect and there is no simple rule on how to set tolerance thresholds. The threshold for sphericity validation that compares the size measured by the two pairs of detectors was set at 30%. This threshold led to the rejection of nearly 65–70% of the detected events, that is, Doppler burst. As we knew that the MVE concerns generally the droplets that are much larger than the measurement volume, it was highly likely that most of the large droplets were eliminated. The

frequency of droplets larger than the measurement volume is almost certainly underestimated in the histograms. However, this problem does not affect the statistical analysis presented in the article. The fitting of the PDF is limited to droplets of sizes not exceeding 250 μm, that is, roughly one third of the measurement volume. We believe that MVE induced a bias that is negligible for these small droplets. Araneo *et al.* [36] investigated the MVE in detail and found that general rules of thumb recommend applying standard phase Doppler techniques for particles with diameters that do not exceed one third or one half the beam waist, which is equal to 600 μm in our experiments. This condition is thus satisfied for the droplets which were the subject of the statistical analysis presented in this article.

Other possible sources of error exist. For example, the PDA technique does not measure the size of the droplets but their radii of curvature in the plane of the detectors (in the case of the present experiments, it was the vertical plane). If the droplets are mostly elongated vertically, then their sizes will be overestimated if we later assume they are spherical. As in the case of the MVE, a rigorous quantification of these errors is difficult, but these errors are likely to affect the bigger droplets with higher Weber numbers. Finally, it should be noted that in the size and velocity ranges of interest in this study, to our knowledge, only the PDA technique can provide size and velocity joint PDF. Even if errors can affect large size droplets, the data is still very relevant for many analyses.

Based on these remarks, a log-stable law was made to fit with the bag number PDF (cf. [16] for the fitting procedure used as a first approach) in the magnitude range [0.8, 2.5]. The result is shown in Fig. 6. In this analysis, the value of the stability parameter is found to be 1.688, which is very close to the experimental value of 1.684 found in [10] for turbulent intermittencies. However, the procedure (i.e., least square method and FFT) used in [10] is quite awkward and does not allow for an easy determination of the uncertainty of the fitting procedure. Therefore, the maximum likelihood estimator procedure devised by Nolan [37] was also used. This resulted in a stability index value equal to 1.70 ± 0.014, where the given uncertainty is related the 95% confidence interval. This new value is closer to the inverse of Flory exponent, found theoretically for turbulence intermittencies ($1/.589 = 1.70$). It should also be noted that the relative uncertainty of the other parameters given by the 95% confidence interval is less than 10%. Using (13) and values (14)–(16), the expected value of the scale parameter for the turbulent dissipation is found to be $\sigma_{\ln\varepsilon} = 2.2$. This fitting of droplets PDF led to a scale parameter $\sigma_{\ln d}$ equal to 1.1, that is, about half the scale parameter of the turbulent dissipation:

$$\sigma_{\ln d} \approx \tfrac{1}{2}\sigma_{\ln\varepsilon}. \tag{17}$$

At first, it seemed rather difficult to relate this new scale parameter to the previous turbulent intermittency scale parameter. It is well known that breakup of the bag leads to the formation of filaments, which then turn into droplets [32]; therefore the volume of the droplets will be in some way related to the size of these filaments. However, the very nature of these filaments remains unknown. As they are seemingly coherent structures, a possible explanation could be that they are composed of vortex filaments resulting from a turbulent vortex cascading mechanism, although this consideration can only be qualitative.

A possible scenario leading to quantitative values was given by Hinze [13,38] when he devised a mechanism of droplet breakup by the turbulence of the carrier phase. It can be easily adapted to a situation where the turbulence inside the (carried) fluid leads to interface creation and to the formation of droplets.

To achieve this, we write that the turbulent dynamic pressure at the surface induced by either inner (or outer, in Hinze analysis) movements is equal to the surface tension pressure of a cylindrical filament of diameter d centered in x (this leads to a turbulent breakup condition for a droplet of diameter d):

$$\frac{1}{2}\rho_L u[(x + d/2) - u(x)]^2 = \frac{\gamma}{d}. \tag{18}$$

Then, using Kolmogorov $4/5^{\text{th}}$ law:

$$d = \left(\frac{2\gamma}{\rho_L}\right)^{3/5}\left(\frac{5}{2}\right)^{2/5}\varepsilon_d^{-2/5}. \tag{19}$$

Therefore,

$$\ln(d) = -\tfrac{2}{5}\ln(\varepsilon) + cst, \tag{20}$$

and the following relation between scale parameters could be expected:

$$\sigma_{\ln d} = \tfrac{2}{5}\sigma_{\ln\varepsilon}. \tag{21}$$

This expression leads to a value of 0.9 for σ_d, whereas 1.1 was measured. The compliance between the values is not perfect, which could be due to the harsh estimates of the different turbulent scales. However, the minus sign in (20) reverses the skew of the stable distribution and predicts that the skew parameter of the distributions of $\ln(d)$ and $\ln(\varepsilon)$ shall be equal but opposite. This is not compatible with our measurements ($\beta_{\ln d} = -1$) and the log-stable turbulence model ($\beta_{\ln\varepsilon} = -1$). Moreover, a simple computation of the order of magnitude in (19) leads to

$$\begin{aligned} d &= \left(\frac{2 \times 0.072}{1000}\right)^{3/5}\left(\frac{5}{2}\right)^{2/5}(5900)^{-2/5} \\ &\approx 221\ \mu\text{m (magnitude 2.3)}. \end{aligned} \tag{22}$$

This gives a good order of magnitude of the Sauter mean diameter of the bag droplets but also indicates that smaller droplets shall be stable. Both these arguments indicate that inner turbulence in the mother droplet cannot be considered to be the mechanism by which the droplets resulting from the bag breakup appear. It should also be noted that considering that turbulent movements of the air lead to the breakup of droplets (i.e., replacing ρ_L by ρ_G as Hinze originally did) leads to a higher value for the droplet diameter in (22).

Therefore, it seems necessary to find another model. Liu and Reitz observed [32] that the breakup of the bag resulted in numerous tiny filaments, which then reorganize into droplets. According to Villermaux and colleagues [38,39], these ligaments may then be covered by small balls (blobs), which add together to make up the volume of the final droplet. Formulating hypotheses about so-called interaction layers, which can be understood as a hypothesis of independence of the size of the covering balls whose radii are supposed to

be exponentially distributed [40], results in a self-convolution process leading to a Gamma PDF (i.e., a product of a power law and an exponential). The conclusion is interesting, but some hypotheses concerning these interaction layers seem questionable [39]. It is known that log-normal PDF can be replaced by Gamma PDF in turbulence modeling [41], but this makes intermittency disappear as the tail of the distribution is much shorter. Unfortunately, since high-speed imaging leads to a limited range of detection in term of droplet sizes, Villermaux and colleagues used a size range around a decade to validate their model. Nevertheless, the physical insights contained in their work seem interesting and may be adapted to analyze the the present bag droplets PDF.

Let us suppose that the fundamental blobs are of radii equal to the Kolmogorov scale and that the "interaction layers" are the results of the agitation by the turbulence of the flow. Since the surface energy needed to form the filament does not appear to come from the turbulent motion, which develops inside the water [cf. (22)], it can be assumed that this energy comes directly from the average kinetic energy of the fluid. In this case, the minimum droplet size would be $d = 2\gamma/\rho U^2 \cong$ 90 nm, far below what is observed. However, this also means that this kind of energy source is potentially able to form any of the tiny droplets created in the burst of the bag.

Let us assume that coherent structures, which develop inside the water ultimately, recess because of an agglomeration process to then form droplets. The size distribution $n(d,t)$ of droplets can be expressed using Smoluchowski's equation [42]:

$$\frac{\partial n(d,t)}{\partial t} = \frac{1}{2}\int_0^d a(d-\xi,\xi)n(d-\xi,t)n(\xi,t)d\xi - n(d,t) \times \int_0^\infty a(d,\xi)n(\xi,t)d\xi, \tag{23}$$

where a is the aggregation kernel. If a is supposed constant, this equation has an analytical solution [43] and the first-order moments of the PDF are given by

$$n(t) = m_0(t) = \frac{n_0}{1 + an_0 t}, \tag{24}$$

$$m_1(t) = d_0[2n_0 - m_0(t)]. \tag{25}$$

In this way, the average length is given by

$$d = \frac{m_1(t)}{m_0(t)} = d_0(1 + 2an_0 t) \approx 2d_0 an_0 t, \tag{26}$$

where d_0 is the initial value of the blobs' diameter or filaments' thickness and n_0 is their initial numeric density per unit volume. Thus, the product of these two quantities can be considered as the cumulated filament length per unit volume.

In the following, the analysis is based on the assumption that the aggregation speed is governed by the gradient of the fluctuating velocity $an_0 \sim \partial u/\partial x \sim \sqrt{\varepsilon/\nu}$, that is, the inverse of Kolmogorov turbulent time τ_η. The aggregation characteristic time is also supposed to be much shorter than the overall aggregation time t, which is set as equal to the turbulent integral time τ_{int} (i.e., aggregation can occur inside the largest eddies). Using standard approximation [35], the integral scale can be written as

$$\tau_{\text{int}} = \frac{L_{\text{int}}}{k^{\frac{1}{2}}} \approx \frac{1350.10^{-6}}{6^{\frac{1}{2}}} = 551\ \mu\text{s}, \tag{27}$$

which, as expected, is much larger than the Kolmogorov time scale given by

$$\tau_\eta = \sqrt{\frac{\nu_G}{\varepsilon}} \approx \sqrt{\frac{1.510^{-5}}{5900}} \approx 50\ \mu\text{s} \tag{28}$$

By using (26), (27) and (28), the droplet size can be expressed as

$$d = \frac{m_1(t)}{m_0(t)} \approx 2d_0\frac{\tau_{\text{int}}}{\tau_\eta} = 2d_0\frac{L_{\text{int}}}{k^{\frac{1}{2}}}\sqrt{\frac{\varepsilon}{\nu_G}} \propto \varepsilon^{\frac{1}{2}}. \tag{29}$$

Therefore the expected $\frac{1}{2}$ scaling between droplet size and turbulent energy dissipation [cf. Eq. (17)] is recovered. It should be noted here that the present model is very close to certain micromixing models developed in chemical engineering [44] where the Kolmogorov time scale is the reference mixing time. In fact, the present modeling was devised *ad hoc* in order to recover this scaling. However, to actually test this dependency is quite difficult as it is hard to make sensitive changes to the turbulence parameters without changing either the atomization device or the atomization regime. An alternative can be used to draw general conclusions, for instance, scaling laws, from the coupling induced by Eq. (17) and to compare them with results available in the literature. This is what is done in the next paragraph.

Scaling laws are numerous in experimental works in atomization, and results are very scattered [12]. In the bag breakup, according to [16,27,28], the size of daughter droplets $d^{(\text{bag})}$ is related to the size of the mother droplet $d^{(\text{init})}$ through the scaling (cf. [45]):

$$\frac{d^{(\text{bag})}}{d^{(\text{init})}} \propto U^{-\frac{1}{2}}, \tag{30}$$

which was derived through a boundary-layer-like analysis. However, data are very scattered, and the limited Reynolds number range that is experimentally available to stay in the bag breakup domain makes Eq. (2) equally valid. Actually scaling (30) can be recovered as previously stated by equating the bag droplet size and the Taylor length scale since $\lambda/L \propto \text{Re}^{-\frac{1}{2}}$ [46]. This is another hint that both average droplet size and Taylor length scale have the same order of magnitude [cf. preceding remarks about Eq. (15)]. A physical interpretation can be found in that Taylor scale is very close do the average distance between instantaneous stagnation points in turbulence [10]. Matter and ligaments enclosed between these stagnation points are likely to reorganize to form the average droplets.

To improve this scaling law by involving turbulence intermittencies, let us recall that knowledge of the Fourier transform (12) makes computation of the moments of the log-stable distribution easy since

$$\langle d^q \rangle = \langle e^{q \ln d} \rangle = \exp\left(q\delta - \frac{\sigma_{\ln d}^\alpha}{\cos\frac{\pi\alpha}{2}}q^\alpha\right). \tag{31}$$

This can be used to compute the scale parameter as

$$\lambda \sim \langle d \rangle = \exp\left(\delta - \frac{\sigma_{\ln d}^{\alpha}}{\cos\frac{\pi\alpha}{2}}\right) \tag{32}$$

and the Sauter mean diameter

$$\ln d_{32} = \ln\left(\frac{\langle d^3\rangle}{\langle d^2\rangle}\right) = \delta - \frac{\sigma_{\ln d}^{\alpha}}{\cos\frac{\pi\alpha}{2}}(3^{\alpha} - 2^{\alpha}). \tag{33}$$

By combining Eqs. (32), (33), and (17), one gets

$$\ln\frac{d_{32}}{L} = -\frac{\sigma_{\ln\varepsilon}^{\alpha}}{\cos\frac{\pi\alpha}{2}}\frac{(3^{\alpha} - 2^{\alpha} - 1)}{2^{\alpha}} + \ln\underbrace{\frac{\lambda}{L}}_{\mathrm{Re}_L^{1/2}}$$

$$= -\frac{1}{2}\ln \mathrm{Re} + \underbrace{\frac{-1}{\cos\frac{\pi\alpha}{2}}\frac{(3^{\alpha} - 2^{\alpha} - 1)}{2^{\alpha}}\frac{1}{4}}_{0{,}19}\ln \mathrm{Re}, \tag{34}$$

which can be rewritten $\frac{d_{32}}{L} = \mathrm{Re}^{-0.31} \approx 1800^{-0.31} \approx 0.1$. Deviation from the exponent 0.5 can be interpreted as a correction due to the intermittencies, and an order of magnitude has been computed for the present case, interestingly leading to a value very close to (2). Note that in the bag breakup regime, integral scale L and mother droplet size $d^{(\mathrm{init})}$ have the same order of magnitude.

Scaling laws are also available for higher Weber number outside the bag-breakup regime. Actually, scalings very different from either (2) or (20) were reported in Lefebvre's book [12]; droplet size decreases as

$$\frac{d_{32}}{d^{(\mathrm{init})}} \propto U^{-\chi}, \tag{35}$$

where exponent χ range, for plain orifice or air-blast atomizer, from around 1 (on the average) to 1.33 (on the maximum). These values of χ, gathered over forty years of different experiments, seem to be very author dependent and tend to increase as new and more precise data acquisition techniques become available. Also of note are data gathered by Ingebo at the US National Aeronautics and Space Administration in the 1980s, which give scaling exponents as high as –1.2 [47] for a jet in a cross flow or –1.33 [48] for an air-blast atomizer.

For high Weber number, the wave number is larger, and the previous description does not apply. The integral scale cannot be confounded anymore with the size of the initial droplet and is more likely to be of the order of magnitude of the unstable wavelength creating the atomization. By combining (3) and (4), this leads to

$$L \propto \lambda_{RT,\,\max} \propto U^{-1}. \tag{36}$$

Finally, one gets $d_{32} \propto U^{-1.31}$, which is very close to the results of Ingebo.

IV. CONCLUSION

In this work, it has been shown that for some high flow-rate industrial sprays, the drop PDF was composed of three peaks in the bag-breakup atomization mechanism. The first two peaks are narrow and respectively correspond to the mother droplet peak and daughter droplet peaks created by burst of the basal ring, or rim of the bag. The sizes of the droplets corresponding to these peaks can be adequately explained by combining Rayleigh-Taylor instability and the droplet distortion and breakup model. An interesting result of this approach is that it accurately predicts the transition between the bag-breakup and the bag-and-stamen or umbrella breakup regimes as well as branching ratio between the rim and the bag breakup. The third peaks related to the bag breakup lead to a very wide range of fragments. The most common size of these fragments can be related to the Taylor scale of turbulent eddies. Taylor-scaled eddies possibly develop inside the droplet during the formation of the bag and its subsequent bursting into numerous filaments. This intuitive idea can be found in previous works by Dai and Faeth [28], but it is currently difficult to assert this fact with certainty. We also underline the fact that it could be equally possible that Taylor-sized eddies, located in the air stream, do indeed act as the main filament reorganization mechanism. This is probably even likelier as orders of magnitude of turbulent fluctuations have been deduced from measurements of droplet global velocities, which are closer to the surrounding air velocities than to the droplet inner flow velocities. Although this does not change the present analysis, it remains an important fundamental question which may soon be answered thanks to recent progress made in the DNS of turbulent two-phase flows [49–51]. Further, the size PDF of the droplets resulting from the burst of the bag complies very well with a log-stable distribution as used in turbulence intermittency modeling, and a possible scenario may be constructed to explain the values of the observed parameters of the distribution and their relative dependency. The value of the stability index is found to be equal to 1.70 as in a recent turbulence intermittency model based on self-avoiding random vortex stretching, the value of the skew parameter is set to –1, and the value of the scale parameter appears to be half the value of the scale parameter of the turbulence energy dissipation distribution. Again, as it is not easy to make big changes to the dynamic range of the turbulence in this experiment, it may be necessary to use direct numerical simulation of these two phase flows as an experimental way to confirm or refute this. This will actually be very close to DNS of Rayleigh-Taylor instability where Kolmogorov scaling is still debated [24], and in a related way, it can be expected that present results could be used to build a semianalytical model of turbulent mixing in the RT instability, as done in [52]. In order to recover scaling published in atomization studies [12,26–28,45,47,48], the value of the shift parameter is set by the Taylor scale of the flow. One of the main advantages of the present modeling is that it does not introduce *in fine* any fitting parameters. Therefore, the proposed framework may help in predicting other atomization mechanisms. Lastly, further refinements of the proposed competition between the deformation of the droplet into a spheroid and the growth of the RT instability will be an interesting sequel to this work.

ACKNOWLEDGMENTS

The authors thank A. Delconte and A. Labergue for their help in data acquisition and B. Oesterlé and F. Lemoine for helpful discussions and comments.

[1] A. N. Kolmogorov, Dokl. Akad. Nauk. SSSR **31**, 99 (1941).
[2] A. M. Obukhov, J. Fluid Mech. **13**, 77 (1961).
[3] A. N. Kolmogorov, J. Fluid Mech. **13**, 82 (1962).
[4] U. Frisch, *Turbulence: The Legacy* of A. N. Kolmogorov (Cambridge University Press, Cambridge, 1995).
[5] D. Schertzer and S. Lovejoy, J. Geophys. Res. **92**, 9693 (1987).
[6] S. Kida, J. Phys. Soc. Jpn. **60**, 5 (1991).
[7] S. Kida, Fluid Dyn. Res. **8**, 135 (1991).
[8] D. Schertzer, S. Lovejoy, F. Schmitt, Y. Chigirinskaya, and D. Marsan, Fractals **5**, 427 (1997).
[9] N. Rimbert and O. Séro-Guillaume, C. R. Mecanique 331 (2003).
[10] N. Rimbert, Phys. Rev. E **81**, 056315 (2010).
[11] P. G. De Gennes, *Scaling Concept in Polymer Physics* (Cornell University Press, Ithaca, NY, 1979).
[12] H. Lefebvre, *Atomization and Sprays* (Taylor & Francis, New York, 1988).
[13] E. A. Novikov and D. G. Dommermuth, Phys. Rev. E **56**, 5479 (1997).
[14] W. X. Zhou and Z. H. Yu, Phys. Rev. E **63**, 016302 (2000).
[15] M. A. Gorokhovski and V. L. Saveliev, Phys. Fluid. **15**, 184 (2003).
[16] N. Rimbert and O. Séro-Guillaume, Phys. Rev. E **69**, 056316 (2004).
[17] M. Gorokhovski and M. Herrmann, Ann. Rev. Fluid Mech. **40**, 343 (2008).
[18] J. Eggers and E. Villermaux, Rep. Progr. Phys. **71**, 036601 (2008).
[19] M. Pilch and C. A. Erdman, Int. J. Multiphase Flow **13**, 741 (1987).
[20] Y. Wang, K. S. Im., and K. Fezzaa, Phys. Rev. Lett. **100**, 154502 (2008).
[21] S. Chandrasekhar, *Hydrodynamic and Hydromagnetic Stability* (Oxford University Press, Oxford, 1961).
[22] C.-L. Ng, R. Sankarakrishnan, and K. A. Sallam, Int. J. Multiphase Flow **34**, 241 (2008).
[23] G. Boffetta, A. Mazzino, S. Musacchio, and L. Vozella Kolmogorov, Phys. Rev. E **79**, 065301(R) (2009).
[24] S. Abarzhi and R. Rosner, Phys. Scr. T **142**, 014012 (2010).
[25] H. E. Albrecht, M. Borys, N. Damaschke, and C. Tropea, *Laser Doppler and Phase Doppler Measurement Techniques* (Springer-Verlag, Berlin, 2003).
[26] W.-H. Chou, L.-P. Hsiang, and G. M. Faeth, Int. J. Multiphase Flow **23**, 651 (1997).
[27] W.-H. Chou and G. M. Faeth, Int. J. Multiphase Flow **24**, 889 (1998).
[28] Z. Dai and G. M. Faeth, Int. J. Multiphase Flow **27**, 217 (2001).
[29] J. Kitschka and G. Kocamustafaogullari, Int. J. Multiphase Flow. **15**, 573 (1989).
[30] P. J. O'Rourke, Ph.D. thesis, Princeton University, 1981 (unpublished).
[31] E. A. Ibrahim, H. Q. Yang, and A. J. Przekwas, AIAA J. Propulsion Power **9**, 651 (1993).
[32] Z. Liu and R. D. Reitz, Int. J. Multiphase Flow **23**, 631 (1997).
[33] D. D. Joseph, J. Belanger, and G. S. Beavers, Int. J. Multiphase Flow **25**, 1263 (1999).
[34] G. Samorodnitsky and M. S. Taqqu, *Stable Non-Gaussian Random Processes* (Chapman and Hall, Boca Raton, FL, 1994).
[35] H. Tennekes and J. L. Lumley, *A First Course in Turbulence* (MIT Press, 1972).
[36] L. Araneo, N. Damaschke, and C. Tropea, Tenth International Symposium on Applications of Laser Techniques to Fluid Mechanics, Lisbon, Portugal, 2000 (unpublished).
[37] J. P. Nolan, in *Lévy Processes: Theory and Application*, edited by O. E. Barndorff-Nielsen, T. T. Mikosch, and S. I. Resnick (Birkhauser, Boston, 2001).
[38] J. O. Hinze, AICHE J. **1**, 289 (1955).
[39] E. Villermaux, Ph. Marmottant, and J. Duplat, Phys. Rev. Lett. **92**, 074501 (2004).
[40] Ph. Marmottant, Ph.D. thesis, l'université Joseph Fourier, 2001 (unpublished).
[41] S. Pope, *Turbulent Flows* (Cambridge University Press, Cambridge, 2000).
[42] M. Smoluchowski, Sitzungsberichte. Abt. 2a, Mathematik, Atronomie, Physik, Meteorologie und Mechanik **123**, 2381 (1914).
[43] D. Ramkrishna, *Population Balances Theory and Applications to Particulate Systems in Engineering* (Academic Press, London, 2000).
[44] R. O. Fox, *Computational Models for Turbulent Reacting Flows* (Cambridge University Press, Cambridge, 2003).
[45] L.-P. Hsiang and G. M. Faeth, Int. J. Multiphase Flow **18**, 635 (1992).
[46] H. Tennekes and J. L. Lumley, *A First Course in Turbulence* (MIT Press, Cambridge, MA, 1972).
[47] R. D. Ingebo, *Capillary and Acceleration Wave Breakup of Liquid Jets in Axial-Flow Airstreams*, NASA Technical Paper 1791 (US GPO, Washington, DC, 1987).
[48] R. D. Ingebo, *Agreement between Experimental and Theoretical Effects of Nitrogen Gas Flowrate on Liquid Jet Atomization*, NASA Technical Memorandum 89821 (US GPO, Washington, DC).
[49] R. Lebas, T. Menard, P. A. Beau, A. Berlemont and F. X. Demoulin, Int. J. Multiphase Flow **35**, 247 (2009).
[50] D. Fuster, G. Agbaglah, C. Josserand, S. Popinet, and S. Zaleski, Fluid Dyn. Res. **41**, 065001 (2009).
[51] J. Shinjo and A. Umemura, Int. J. Multiphase Flow **36**, 513 (2010).
[52] U. Alon, J. Hecht, D. Mukamel, and D. Shvarts, Phys. Rev. Lett **72**, 2867 (1994).